



## Original Research

## Assessment of an scFv Antibody Fragment Against ELTD1 in a G55 Glioblastoma Xenograft Model☆☆☆

Michelle Zalles<sup>a,b</sup>, Nataliya Smith<sup>a</sup>, Debra Saunders<sup>a</sup>, Tanvi Saran<sup>a</sup>, Lincy Thomas<sup>a,c</sup>, Rafal Gulej<sup>a,d</sup>, Megan Lerner<sup>e</sup>, Kar-Ming Fung<sup>f,g</sup>, Junho Chung<sup>h</sup>, Kyusang Hwang<sup>h</sup>, Junyeong Jin<sup>h</sup>, James Battiste<sup>b,g,i</sup>, Rheal A. Towner<sup>a,f,b,g,\*</sup>

<sup>a</sup> Advanced Magnetic Resonance Center, Oklahoma Medical Research Foundation, Oklahoma City, OK, USA

<sup>b</sup> Oklahoma Center for Neuroscience, Medical University of Lodz, Lodz, Poland

<sup>c</sup> The Jimmy Everest Center for Cancer and Blood Disorders in Children, Medical University of Lodz, Lodz, Poland

<sup>d</sup> Pharmaceutical Department, Medical University of Lodz, Lodz, Poland

<sup>e</sup> Surgery Research Laboratory, Medical University of Lodz, Lodz, Poland

<sup>f</sup> Department of Pathology, Medical University of Lodz, Lodz, Poland

<sup>g</sup> Stephenson Cancer Center, Medical University of Lodz, Lodz, Poland

<sup>h</sup> Department of Biochemistry and Molecular Biology, Seoul National University College of Medicine, Seoul, Republic of Korea

<sup>i</sup> Department of Neurology, Medical University of Lodz, Lodz, Poland



## ARTICLE INFO

## Article history:

Received 27 September 2019

Received in revised form 11 December 2019

Accepted 12 December 2019

Available online xxx

## Keywords:

Glioblastoma (GBM)

ELTD1

Angiogenesis

Orthotopic G55 xenograft model

MRI

single chain variable fragment (scFv)

## ABSTRACT

Glioblastoma (GBM), the most common primary brain tumor found in adults, is extremely aggressive. These high-grade gliomas, which are very diffuse, highly vascular, and invasive, undergo unregulated vascular angiogenesis. Despite available treatments, the median survival for patients is dismal. ELTD1 (EGF, latrophilin, and 7 transmembrane domain containing protein 1) is an angiogenic biomarker highly expressed in human high-grade gliomas. Recent studies have demonstrated that the blood-brain barrier, as well as the blood-tumor barrier, is not equally disrupted in GBM patients. This study therefore aimed to optimize an antibody treatment against ELTD1 using a smaller scFv fragment of a monoclonal antibody that binds against the external region of ELTD1 in a G55 glioma xenograft glioma preclinical model. Morphological magnetic resonance imaging (MRI) was used to determine tumor volumes and quantify perfusion rates. We also assessed percent survival following tumor postdetection. Tumor tissue was also assessed to confirm and quantify the presence of the ELTD1 scFv molecular targeted MRI probe, as well as microvessel density and Notch1 levels. In addition, we used molecular-targeted MRI to localize our antibodies *in vivo*. This approach showed that our scFv antibody attached-molecular MRI probe was effective in targeting and localizing diffuse tumor regions. Through this analysis, we determined that our anti-ELTD1 scFv antibody treatments were successful in increasing survival, decreasing tumor volumes, and normalizing vascular perfusion and Notch1 levels within tumor regions. This study demonstrates that our scFv fragment antibody against ELTD1 may be useful and potential antiangiogenic treatments against GBM.

□ Funding: Funding was provided in part by the Oklahoma Medical Research Foundation (R.T.), the Seoul National University Foundation (J.C.), and the National Institutes of Health (1S10OD023508-01 to R.T). Whole slide scanning and image analysis are kindly provided by Peggy and Charles Stephenson Cancer Center at the University of Oklahoma Health Sciences Center, Oklahoma City, OK; an Institutional Development Award from the National Institute of General Medical Sciences (P20 GM103639); and a Cancer Center Supporting Grant Award from the National Cancer Institute (P30 CA225520).

□ Conflict of interest: None of the authors have any conflict of interest.

\* Address all correspondence to: Rheal A. Towner, Ph.D., Director, Advanced Magnetic Resonance Center, Oklahoma Medical Research Foundation, 825 NE 13th St., Oklahoma City, OK 73104, USA.

E-mail address: [Rheal-Towner@omrf.org](mailto:Rheal-Towner@omrf.org). (R.A. Towner).

## Introduction

Glioblastoma (GBM) accounts for 60-70% of all diagnosed malignant gliomas in adults [1]. WHO Grade IV GBM can be subclassified as primary tumors that arise from normal glial cells seen in older patients and secondary tumors which are less common and arise from a progression of lower-grade tumors seen in younger patients [2]. Although these two subclasses are histologically identical, primary GBM accounts for approximately 95% of all GBM cases, while the remaining 5% account for secondary GBM [3]. The median age for diagnosis is around 64 years of age, and while there is no verified genetic correlation, about 5% of patients had a family history of glioma diagnosis [4]. The standard treatment of care for GBM is surgical resection to remove the bulk tumor, followed by a combination of radiation and chemotherapy to combat the remaining cancer

cells; however, this treatment plan has not significantly increased the survival of patients post detection. Temozolomide (TMZ) is the most common chemotherapeutic agent used and has increased the overall median survival from 12-15 months [5]. TMZ is an alkylating agent that is able to cross the blood-brain barrier (BBB) and works to produce breaks along the DNA double strand that results in the death of the tumor cells [6]. However, patients whose tumor cells have high O<sup>6</sup>-methylguanine-DNA methyltransferase expression have been demonstrated to be resistant to the cytotoxic activity of TMZ [7]. Bevacizumab is a monoclonal antibody treatment against vascular endothelial growth factor-A (VEGF-A) that has been used in multiple different cancers (colon, lung, and cervix) to target and inhibit the formation of new blood vessels within the tumor region. This therapeutic was fast-tracked and approved by the FDA in 2009 after successful Phase 2 clinical trials in recurrent glioblastomas [8,9]. However, when administered to newly diagnosed patients in combination with the standard treatment plan, bevacizumab had no effect on patient survival [10].

GBM is a diffuse glioma derived from astrocytes and is characterized by its high degree of invasiveness, diffusiveness, and prolific angiogenesis, making this cancer difficult to treat. GBMs have perfected various mechanisms to robustly increase the formation of blood vessels within the tumor environment. One of these mechanisms is the sprouting of capillaries from preexisting blood vessels, which is dependent on the hypoxic environment in the tumor core. Hypoxia occurs frequently in solid tumors because of increased cell proliferation and is most commonly detected through magnetic resonance imaging (MRI) where the areas show decreased or absent blood flow [11]. From this tumor core, molecular markers of hypoxia, such as the hypoxia-inducible factor 1, work to increase the expression of the proangiogenic markers VEGF, Notch1, Notch4, and Hey1 [12,13]. In normal vasculature, the VEGF binds onto its receptor, VEGFR2. The activation of this receptor then stimulates DLL4 to inhibit Notch as well as the lateral growth of vessels [14]. However, in GBM, the excessive amounts of proangiogenic cytokines secreted overcome antiangiogenic factors which in turn form a vascular network to transport nutrients and drive tumor growth.

For various years, VEGF and Notch were two of the most studied pathways in GBM and were accredited to being the major drivers behind angiogenesis. However, in recent years, the epidermal growth factor latrophilin and seven transmembrane domain containing protein on chromosome 1 (ELTD1), alternatively known as the adhesion G protein-coupled receptor L4, were found to be novel regulators of brain angiogenesis and sought to promote metastasis and tumor growth [15]. Although first discovered in developing cardiomyocytes, ELTD1 is highly expressed on both endothelial and tumor cells in high-grade gliomas, such as GBM [16,17]. Interestingly, in normal vasculature, ELTD1 expression was decreased by the DLL4/Notch signaling pathway, and VEGF was found to increase ELTD1 expression [15].

Due to the increased angiogenesis within the tumor, the brain tumor capillaries form a barrier known as the blood-brain tumor barrier (BBTB) [18]. Although the tight junctions in the BBB become leaky, the BBTB may, in some patients, remain intact, therefore creating another barrier for drug delivery. Furthermore, MRI contrast enhancement has suggested that although the BBTB may become leaky, this does not signify that the disruption of the barrier is sufficient enough for drug penetration into the tumor [18]. Due to the BBB and BBTB limitations on drug entry, researchers have looked for smaller therapeutic treatments, including antibodies. While most research has been focused on full polyclonal or monoclonal antibodies, smaller antibody components, like single-chain variable fragments (scFvs), have become increasingly attractive to reduce size [19,20].

In this present study, we aimed to optimize an antibody treatment against ELTD1 using an scFv antibody fragment of a monoclonal antibody (mAb) that binds against the 430 AA external region of ELTD1 in a G55 glioma xenograft glioma preclinical model. We used morphological MRI to assess tumor volumes, and perfusion imaging to measure vascular changes, following either ELTD1 scFv or mAb treatments in tumor regions. Animal survival was also determined following scFv or mAb treatments. Through the use of molecular targeted (mt)-MRI, we assessed the binding affinity and specificity of an anti-ELTD1 scFv fragment probe.

## Methods

### *Preparation of Recombinant Extracellular Domain of ELTD1 Human C<sub>κ</sub> Fusion Protein*

To construct the extracellular domain of human ELTD1 and mouse ELTD1 expression vectors, genes encoding the human ELTD1 (Glu20-Leu406) and mouse ELTD1 (Glu20-Leu455) were chemically synthesized (Genscript, Piscataway, NJ). The genes were subcloned into the modified pCEP4 vector encoding C<sub>κ</sub> domain (human immunoglobulin κ light chain constant domain) at the 5' region as reported previously [21].

The expression vectors encoding the extracellular domain of human ELTD1 and mouse ELTD1 were transfected into HEK293F cells (Invitrogen, Carlsbad, CA) using 25-kDa linear polyethyleneimine (Polyscience, Warrington, PA), as reported previously [22]. Human and mouse ELTD1 C<sub>κ</sub> fusion proteins were purified from the culture supernatants by affinity chromatography using KappaSelect resin (GE Healthcare) according to the manufacturer's instructions.

### *Generation of Anti-ELTD1 Antibody*

White leghorn chickens were immunized with human ELTD1 C<sub>κ</sub> fusion proteins. A phage-displayed chicken scFv library was constructed using total RNA isolated from the bone marrow, spleen, and bursa of Fabricius of immunized chickens, as described previously [23]. Positive clones were enriched by biopanning and screened in a phage enzyme immunoassay, as described previously [24]. Phage clones showing cross-reactivity against human and mouse ELTD1 were selected, and their nucleotide sequences were determined by Sanger sequencing.

The gene of selected scFv clone was subcloned into a modified mammalian expression vector encoding the hinge region of human IgG1 and the CH2-CH3 domains of rabbit IgG at the 3' region as reported previously [25]. The expression vectors encoding anti-ELTD1 scFv-rFc fusion were transfected into HEK293F cells (Invitrogen) as described above. The scFv-rFc fusion protein was purified from the culture supernatants of transiently transfected HEK293F cells using protein A Sepharose column (Repligen, Waltham, MA) according to the manufacturer's instructions.

### *Enzyme Immunoassay*

Ninety-six-well microtiter plate wells (Corning Inc., Corning, NY) were coated with human ELTD1 or mouse ELTD1 C<sub>κ</sub> fusion protein in coating buffer (0.1 M NaHCO<sub>3</sub>, pH 8.6) and then blocked with 3% (w/v) BSA in phosphate-buffered saline (PBS). After incubation with serially 10-fold diluted anti-ELTD1 scFv-rFc fusion protein (0.01-100 nM), horseradish peroxidase (HRP)-conjugated goat anti-rabbit IgG (Fc specific) (Jackson Immuno Research, Inc., West Grove, PA) was added to each well. After washing with 0.05% (v/v) Tween 20 in PBS (PBST), ABTS HRP substrate solution (Thermo-Scientific Pierce, Rockford, IL) was added, and the absorbance was measured at 405 nm with a Multiscan Ascent microplate reader (LabSystems, Helsinki, Finland).

### *G55 Xenograft Model and Treatment*

All animal studies were conducted with the approval (protocol 17-48) of the Oklahoma Medical Research Foundation Institutional Animal Care Use Committee policies, which follow NIH guidelines. Human G55 xenograft cells were implanted intracerebrally in 2-month-old male athymic nude mice (Hsd:Athymic Nude-Foxn1nu mice; Harlan Inc., Indianapolis, IN). The anesthetized mice were placed and immobilized on a stereotaxic unit. (Stoelting Co., Wood Dale, IL). Aseptic surgery techniques were used, and a 1-mm burr hole was drilled into the skull of the animal 2 mm anterior, 1.5 mm lateral to the bregma on the right side. A 20-μl gas-tight Hamilton syringe was used to inject (1 × 10<sup>4-5</sup>) G55 cells per ml (suspended in 4 μl of cell culture media with 1% agarose) into the right

frontal lobe at a depth of 2.5 mm relative to the dural surface in a stereotaxic unit. The cell lines were maintained and expanded immediately prior to inoculation and not used for more than 10 passages. Following injection, the skin was closed with surgical sutures (monofilament, absorbable). Buprenex (i.p. injection) was administered to the animal following cell implantation procedure for pain relief during recovery. The animals were divided into three groups: untreated, mAb (monoclonal antibody) against ELTD1, and scFv fragment of the mAb against ELTD1. Once tumors reached 6-7 mm<sup>3</sup> (determined via MRI), mice were treated with 2 mg/kg of either optimized mAb against ELTD1 or the scFv fragment of mAb against ELTD1 every 3-4 days (treated M/Th, T/F, W/Sat) until the tumors reached 150mm<sup>3</sup>, or were left as untreated controls. All mice were euthanized when tumors reached ≥ 150 mm<sup>3</sup> prior to tumor-induced death.

*In Vivo MR Techniques*

*Morphological Imaging*

Mice were anesthetized and positioned in a cradle. A 30-cm horizontal bore Bruker Biospin magnet operating at 7 T (Bruker BioSpin GmbH, Karlsruhe, Germany) was used. A BA6 gradient set and mouse head coil were used to perform all MRI experiments as previously described [26]. All animals were imaged every 3-4 days (M/Th, T/F, W/Sat) until the end of the study starting at 10 days post-G55 implantation surgery.

*Perfusion Imaging*

The perfusion imaging method, arterial spin labeling (ASL), was used as previously described [27]. Perfusion maps were obtained on a single axial

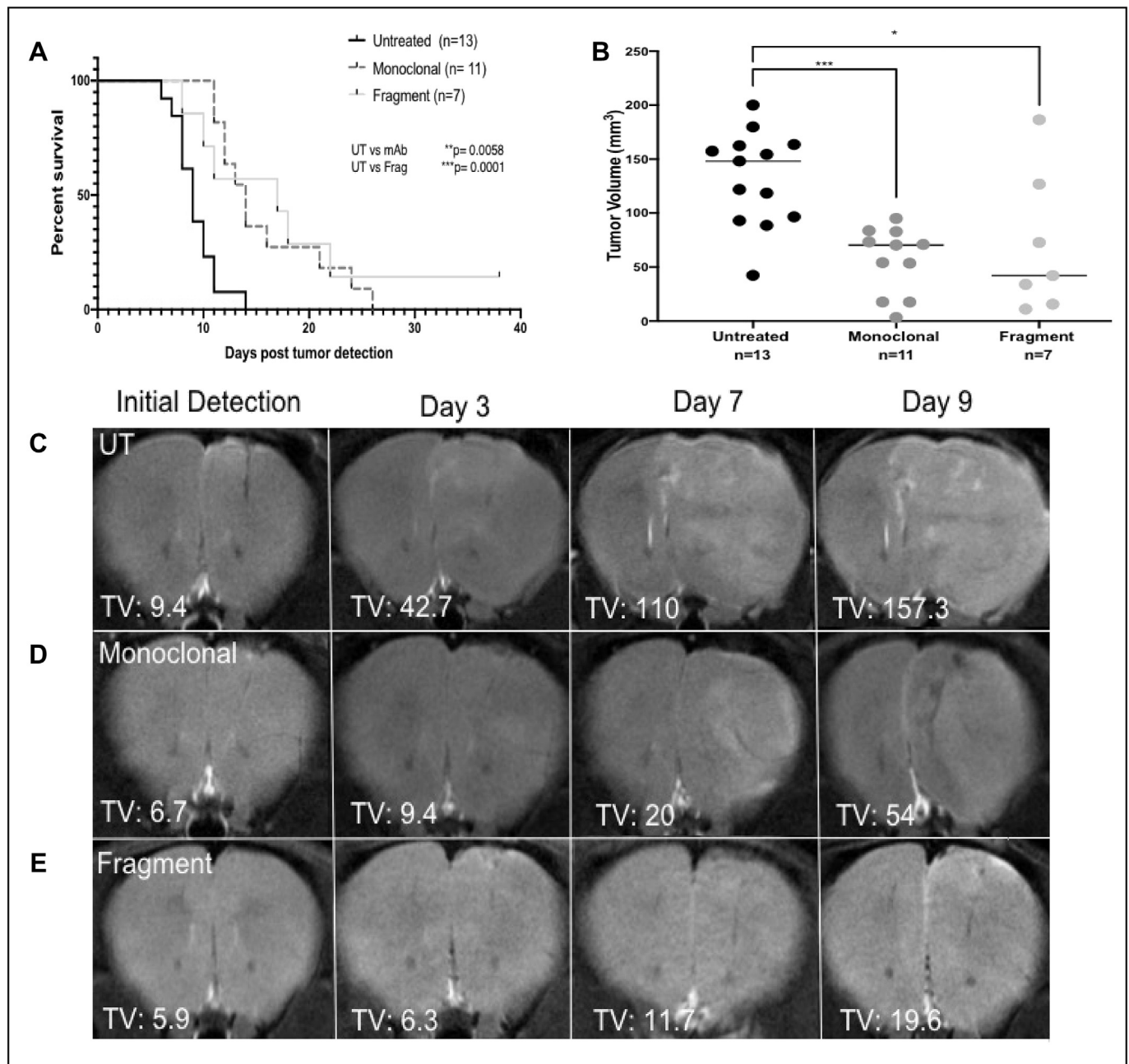


**Figure 1.** Anti-ELTD1 treatments were successful in increasing percent survival post tumor detection as well as decreasing tumor volumes. (A) The antibody treatment against ELTD1, both monoclonal (\*\*P = .0058) and fragment (\*\*\*P = .0001), significantly increased the tumor percent survival compared to UT control (average survival 9 days) as shown in the percent survival curve. (B) Tumor volumes were also found to be significantly lower with the monoclonal (\*P = .0009) and fragment (\*P = .017) anti-ELTD1 treatment compared to untreated animals. Also shown are the representative morphological tumor images of untreated (C), monoclonal-treated (D), and fragment-treated (E) mice. Time points include initial detection (day 0) and days 3, 7, and 9 following detection. For each time point, relevant tumor volumes (TV) are included.

slice of the brain located on the point of the rostrocaudal axis where the tumor had the largest cross section. Five regions of interest (ROIs) were manually outlined around the tumor, and appropriate ROIs were also taken from the contralateral side of the brain for comparison purposes. To calculate the differences in [relative cerebral blood flow (rCBF)] values, tumor rCBF values were obtained at late (prior to termination) and early (at tumor detection) tumor stages and normalized to rCBF values in the contralateral brain region of corresponding animals.

#### mt-MRI

The contrast agent, biotin-BSA (bovine serum albumin)-Gd (gadolinium)-DTPA, was prepared as previously described by our group [26] based on the modification of the method developed by Dafni et al. [28,29]. mAb or scFv fragment anti-ELTD1 was conjugated to the albumin moiety through a sulfo-NHS-EDC link according to the protocol of Hermanson [30]. mt-MRI was performed when tumor volumes were around 130-180 mm<sup>3</sup>. Molecular probes with a biotin-albumin-Gd-DTPA construct bound to anti-ELTD1 antibodies were injected via a tail vein catheter in mice. A nonspecific mouse immunoglobulin IgG Ab (Alpha Diagnostics) was used with the biotin-albumin-Gd-DTPA construct as a negative control. MRI was done as previously described [28,31]. Relative probe concentrations were calculated to assess the levels of ELTD1 and the nonspecific IgG contrast agent in each animal. Contrast difference images were created from the pre- and (90 minutes) postcontrast datasets for the slice of interest by computing the difference in  $T_1$  relaxation times between the postcontrast and the precontrast image on a pixel basis. From difference images, 10 ROIs of equal size (0.05 cm<sup>2</sup>) were drawn within areas with the highest  $T_1$  relaxation at the TR 800 ms, in the tumor parenchyma and contralateral side of the brains of each animal, after anti-ELTD1 probe injections.  $T_1$  values obtained from the ROIs in the tumor regions were normalized to the corresponding contralateral sides. The  $T_1$  relaxation values of the specified ROIs were computed from all pixels in the ROIs by the following equation (processed by ParaVision 5.0, Bruker):  $S(TR) = S_0(1 - e^{-TR/T_1})$ , where TR is the repetition time,  $S_0$  is the signal intensity (integer machine units) at TR,  $T_1$  and TE = 0, and  $T_1$  is the constant of the

longitudinal relaxation time [32]. Overlays of contrast difference images and  $T_1$ -weighted images were generated using Photoshop software (version C.S 6).

#### Immunohistochemistry and Standard Staining

All mice were euthanized after the last MRI examination or when tumors reached 150 mm<sup>3</sup>. The brain of each animal was removed, preserved in 10% neutral buffered formalin, and processed routinely. Hematoxylin-eosin staining: Tissues were fixed in 10% neutral buffered formalin, dehydrated, and embedded in paraffin. Sections were deparaffinized, rehydrated, and stained according to standard protocols. Several reagents were produced by Vector Labs Inc. (VLI) in Burlingame, CA.

Histological sections (5  $\mu$ m) embedded in paraffin and mounted on HistoBond Plus slides (Statlab Medical Products, Lewisville, TX) were rehydrated and washed in PBS. The sections were processed using the ImmPRESS VR Reagent Anti-Rabbit IgG Peroxidase (VLI cat. #MP-6401). Antigen retrieval (pH 6 citrate antigen unmasking solution; VLI cat. #H-3300) was accomplished via 20 minutes in a steamer followed by 30-minute cooling at room temperature. Sections were treated with a peroxidase blocking reagent (Bloxall, VLI cat. #SP-6000) followed by 2.5% normal horse serum to inhibit nonspecific binding. Rabbit Anti-CD34 antibody (abcam 81289; 5.28  $\mu$ g/ml; Cambridge, MA) or Rabbit Anti-NOTCH 1 (abcam 52627; 11  $\mu$ g/ml; Cambridge, MA) was applied to each section, and following incubation overnight (4°C) in a humidified chamber, sections were washed in PBS; the ImmPRESS VR reagent was applied according to the manufacturer's directions.

To characterize MVD and Notch expression levels, five ROIs, captured digitally (20 $\times$ ), were identified in each case. Only areas containing tumor tissue were analyzed, excluding areas with necrosis and/or significant artifacts. The number of positive pixels was divided by the total number of pixels (negative and positive) in the analyzed area. ROIs were analyzed and imaged using Aperio ImageScope (Leica Biosystems, Buffalo Grove, IL).

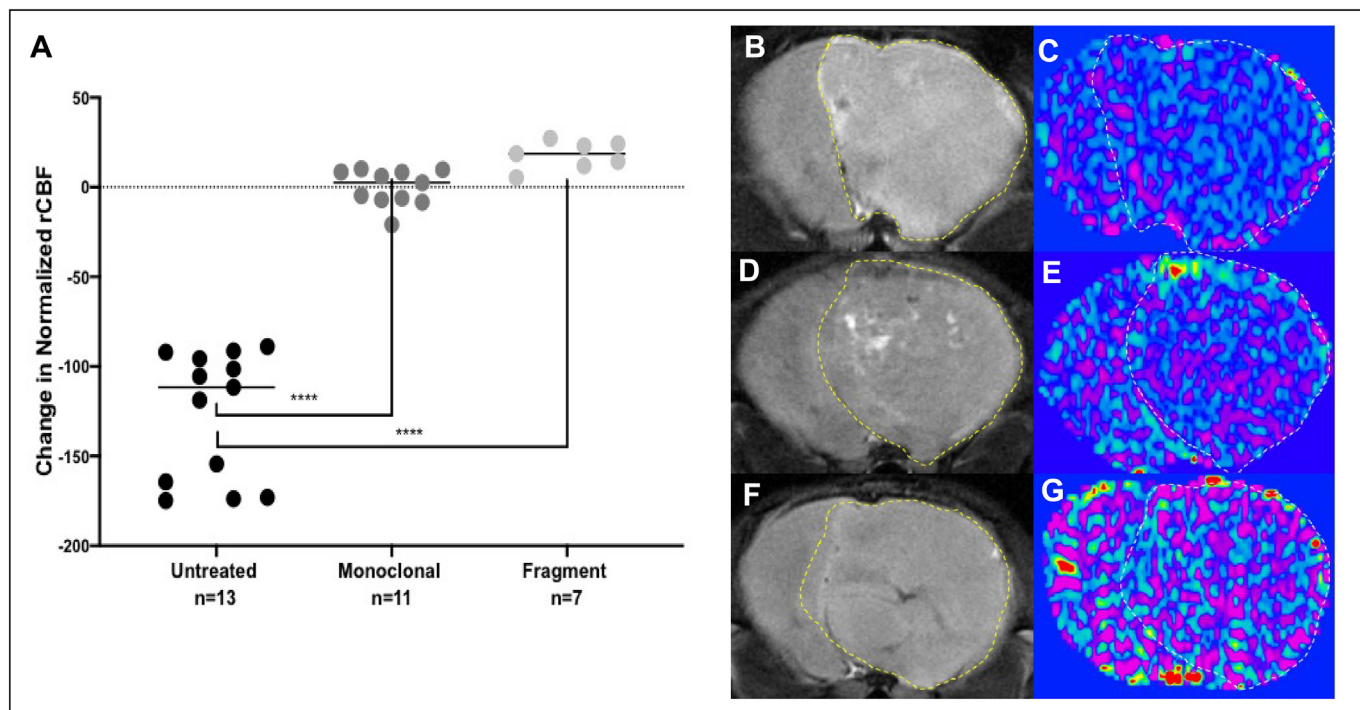


**Figure 2.** rCBF was normalized with the anti-ELTD1 treatments. (A) The monoclonal and fragment anti-ELTD1 treatments were significantly more effective in minimizing the decrease in the rCBF (\*\*\*\* $P < .0001$ ) compared to untreated mice. Representative morphological image and perfusion maps (colorized) for each treatment group: untreated (B, C), monoclonal (D, E), and fragment (F, G).

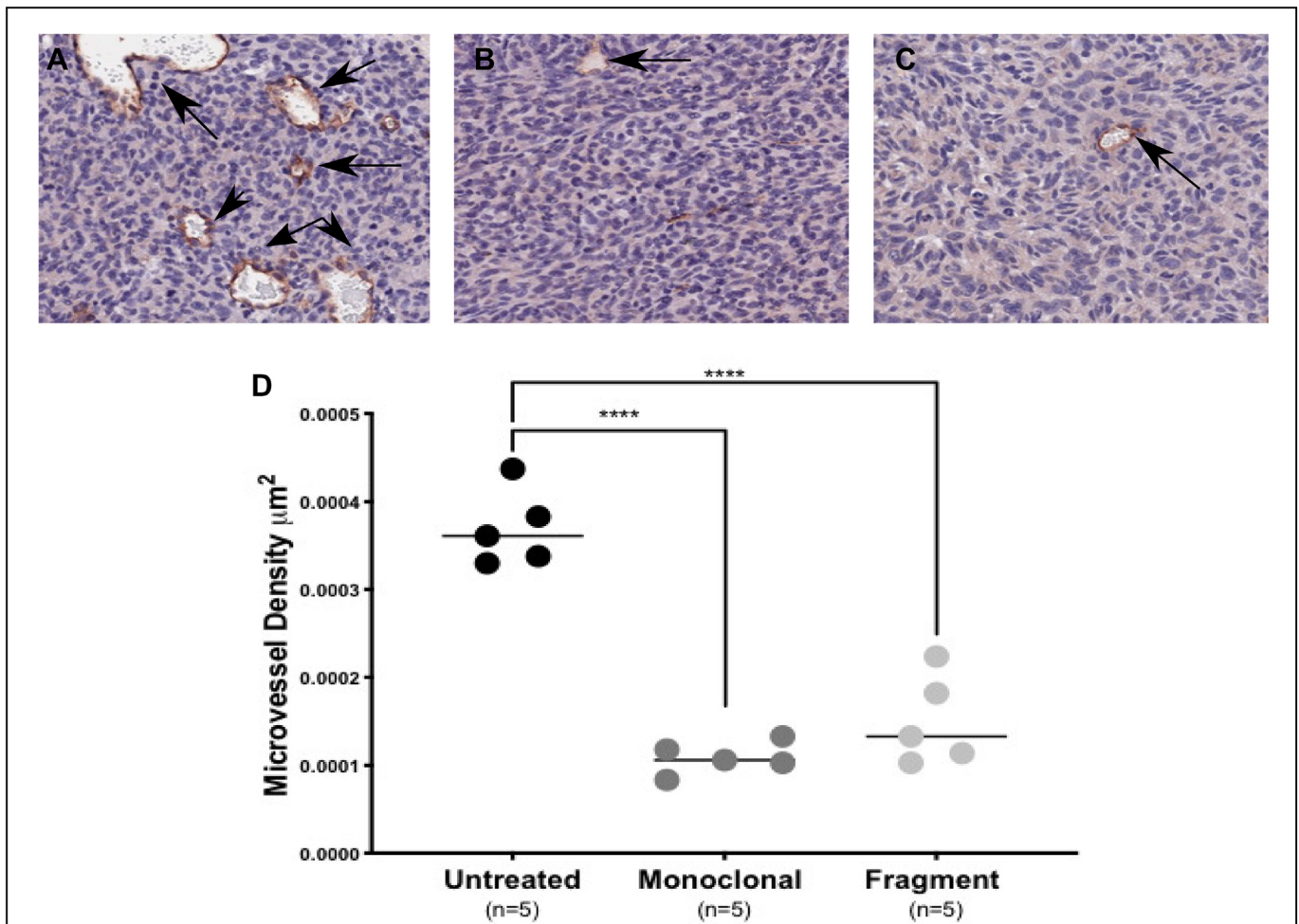


**Figure 3.** Anti-ELTD1 significantly decreased tumor associated vasculature. MVD was analyzed with Aperio ImageScope for the treatment groups. Representative IHC images (20×) of CD34 staining for all treatment groups: untreated (A), mAb (B), fragment (C). Arrows are pointing to the vessels found in the tumor region. (D) Both mAb and fragment treatments against ELTD1 significantly decreased microvessel densities within the tumor region (\*\*\**P* < .0001).

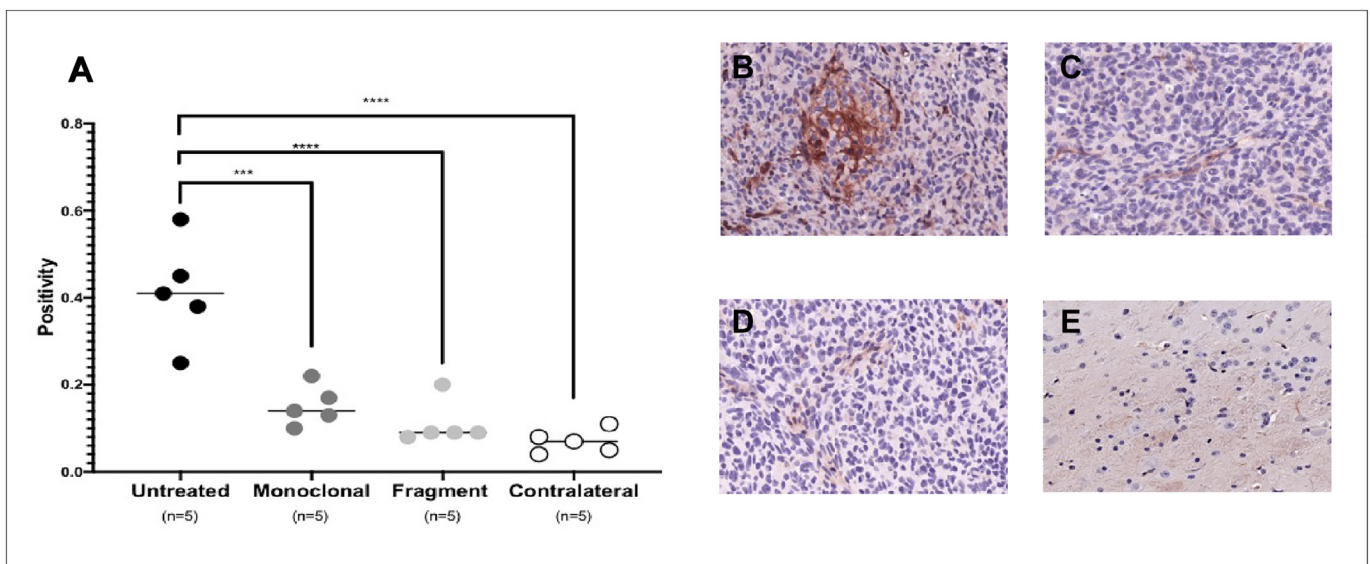


**Figure 4.** Anti-ELTD1 treatments decreased Notch1 levels. Notch1 positivity was analyzed with Aperio ImageScope for the treatment groups (A) Notch1 positivity staining for all treatment groups. Contralateral tissue had significantly decreased Notch1 staining compared to UT. Both anti-ELTD1 treatments were successful in decreasing and normalizing Notch1 levels to those seen in contralateral tissue. Representative IHC images (20×) of Notch1 staining of untreated tissue (B), mAb treatment tissue (C), fragment treatment tissue (D), and contralateral control tissue (E) (\*\*\**P* = .0001, \*\*\*\**P* < .0001).

Sections for SA-HRP were processed as above, except they were incubated overnight with R.T.U. Strp-HRP (VLI cat. #SA-5704). Appropriate washes were in PBS. Slides were incubated with NovaRed (VLI cat. #SK-4805) chromogen for visualization. Counterstaining was carried out with Hematoxylin QS Nuclear Counterstain (VLI). Appropriate positive and negative tissue controls were used.

### Statistical Analysis

Survival curves were analyzed using Kaplan-Meier curves. Tumor volumes, perfusion changes, and immunohistochemistry protein levels, and molecular-targeted MRI data were analyzed and compared by one- or two-way ANOVA with multiple comparisons (Tukey's or Sidak's, respectively). Data were represented as mean  $\pm$  SD, and  $P$  values of either  $* < .05$ ,  $** < .01$ ,  $*** < .001$ , or  $**** < .0001$  were considered statistically significant.

### Results

We intracerebrally implanted human G55 cells into 2-month old male athymic nude mice. Tumor growth was monitored via morphological MRI, and upon tumor detection (6-7 mm<sup>3</sup>), treatments were administered every 3-4 days via tail vein with either the monoclonal anti-ELTD1 antibody or scFv (also referred to as fragment in this manuscript) against ELTD1. The percent survival post tumor detection of G55-glioma-bearing

mice was significantly higher with both the mAb ( $*P = .0058$ ) and fragment ( $***P = .0001$ ) treatment as depicted in Figure 1A. The untreated group had an average survival of 9 days, and therefore, we compared the tumor volumes at day 9 post tumor detection. Tumor volumes at 9 days post tumor detection were significantly lower with the anti-ELTD1-treated mice (mAb  $***P = .0009$ ; fragment  $*P = .017$ ) when compared with untreated controls (Figure 1B). Representative MRIs of G55 tumor-bearing mice from all treatment groups are shown in Figure 1, C-E.

Anti-ELTD1 treatment targets angiogenesis; therefore, we wanted to examine if the treatments had an effect on the microvasculature. Tumor microvascular changes associated with tumor angiogenesis can be measured through the decrease of rCBF. As the vasculature within the tumor region grows, it exponentially becomes more chaotic, therefore decreasing the perfusion rate. Perfusion scans performed with MRI demonstrated a characteristic decrease in rCBF in the tumor region of untreated animals (Figure 2A). The perfusion values in mice treated with anti-ELTD1 treatments were significantly improved when compared to untreated ( $P < .0001$  for both). The monoclonal antibody treatments had a normalization of perfusion values, while the fragment-treated animals had an increase of perfusion (Figure 2A). Figure 2, C, E, G shows representative perfusion scans for each group. The untreated perfusion scan has distinct dark regions only within the tumor region (outlined by the yellow dashed line) depicting the decrease in perfusion within the region. However, the tumor regions in the perfusion scans of the monoclonal and fragment treated mice are homologous with the contralateral tissue. Furthermore, we sought to

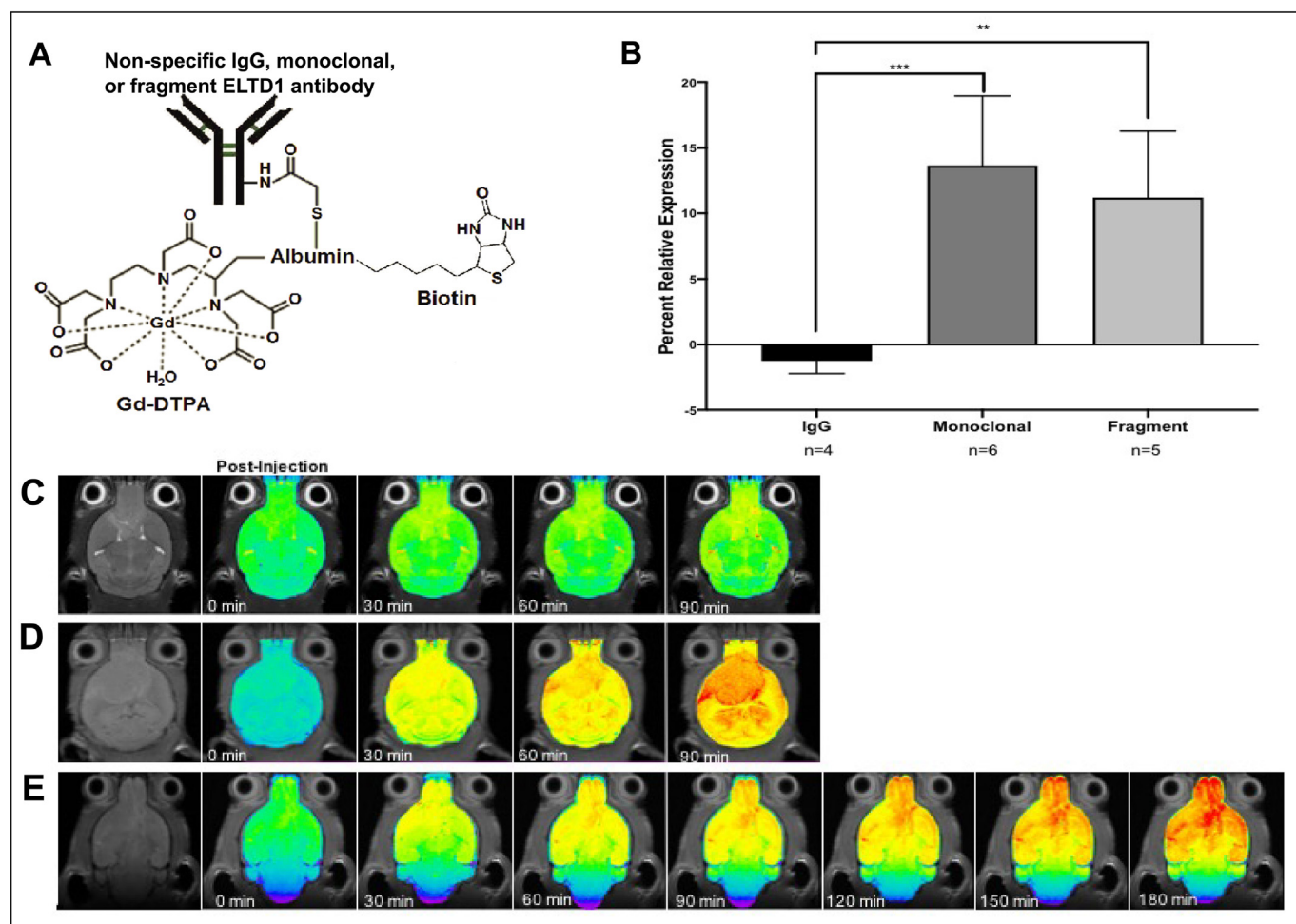


**Figure 5.** ELTD1 antibody attached probes were successful in reaching and infiltrating the tumor region. (A) Construct of the molecular targeting probe attached with either nonspecific IgG, monoclonal, or fragment ELTD1 Ab. (B) Signal intensity was significantly increased by the monoclonal and fragment anti-ELTD1 attached probe ( $**P = .0038$ ,  $***P = .0007$ ). Binding affinity of the (C) nonspecific IgG contrast agent construct, (D) monoclonal attached probe (both over 90 minutes), and the (E) fragment attached probe (over the course of 180 minutes).

characterize the effect of our anti-ELTD1 treatment on the tumor associated vasculature. Both of the anti-ELTD1 therapies sought to significantly decrease the microvessel density (MVD) levels ( $P < .0001$ ) in the tumor region when compared to control (Figure 3D). Representative CD34 IHC images for all of the treatment groups are shown in Figure 3, A-C.

ELTD1 expression has been demonstrated to be upregulated by VEGF and downregulated by Notch/DLL4 in normal vasculature [33]. In previous studies, we have examined the relationship between VEGF and ELTD1 and discovered that, by targeting ELTD1, VEGFR2 levels were decreased in a glioma model [31]. Therefore, in this study, we sought to determine if our antibody treatment had an effect on Notch. Tissue from glioma-bearing mice from each group was stained with Notch1, and the positivity was analyzed. We sought to characterize the difference in Notch1 positivity levels between the tumor region and contralateral tissue. Figure 4A demonstrates that the positivity levels in the contralateral tissue were significantly lower ( $P < .0001$ ) when compared to the levels in the tumor region. Furthermore, our monoclonal and fragment anti-ELTD1 treatments were successful in significantly decreasing Notch1 levels ( $P = .0001$  and  $P < .0001$ , respectively) within the tumor region and were able to bring them down to contralateral levels (Figure 4A). Representative tissue images shown in Figure 4, B-E depict the decreased Notch1 staining within the anti-ELTD1-treated tumor regions.

To determine whether our antibody treatments were crossing the BBB and were responsible for the previous results shown above, we attached either nonspecific IgG, monoclonal anti-ELTD1 or the scFv fragment onto our molecular probe previously described (albumin-biotin-Gd-DTPA) and shown in Figure 5A [28]. The molecular probes were injected via tail vein into untreated glioma-bearing animals and were monitored via MR

molecular targeting imaging. The Gd-DTPA attached onto our molecular probe allows us to determine where our molecular probe is attaching and allows us to quantify the amount of signal intensity within the tumor region. Figure 5, B, C demonstrates that the nonspecific IgG attached probe was a suitable control because the signal intensity was at baseline after 90 minutes. Differences in signal intensity, however, were significantly higher for the monoclonal and fragment attached molecular probes shown in Figure 5B ( $P = .0007$  and  $P = .0038$ , respectively). Furthermore, Figure 5D demonstrates how the monoclonal anti-ELTD1 attached probe localized within the tumor region over the course of 90 minutes. The scFv fragment had slightly decreased signal intensity 90 minutes postinjection; therefore, we decided to examine the binding of the molecular probe for up to 180 minutes. Figure 5E demonstrates that the fragment attached probe requires a longer time to bind onto and localize in the tumor region.

Our fragment-attached probe did not only localize in the bulk tumor seen through MRI but instead bound around other regions thought initially not to be tumor tissue, as seen in the last frame of Figure 5E. The glioma tissue was then stained with SA-HRP, which binds onto the biotin tag attached on the molecular probe, to further examine the regions that the probe bound to. Our fragment-attached probe was successful in reaching the bulk tumor as shown through SA-HRP staining shown in the top voxel in Figure 6. Furthermore, H&E analysis of the tissue discovered that there were extremely diffuse tumor regions along the lateral cortex regions of the brain, which our probe successfully bound onto, as shown in the last frame of Figure 5E. We were also able to find our molecular probe through SA-HRP staining in the diffuse tumor regions as seen in the bottom right region in Figure 6, C, D, in addition to the primary tumor (Figure 6, A, B). Comparative 'normal' brain regions are also shown (Figure 6, E, F).

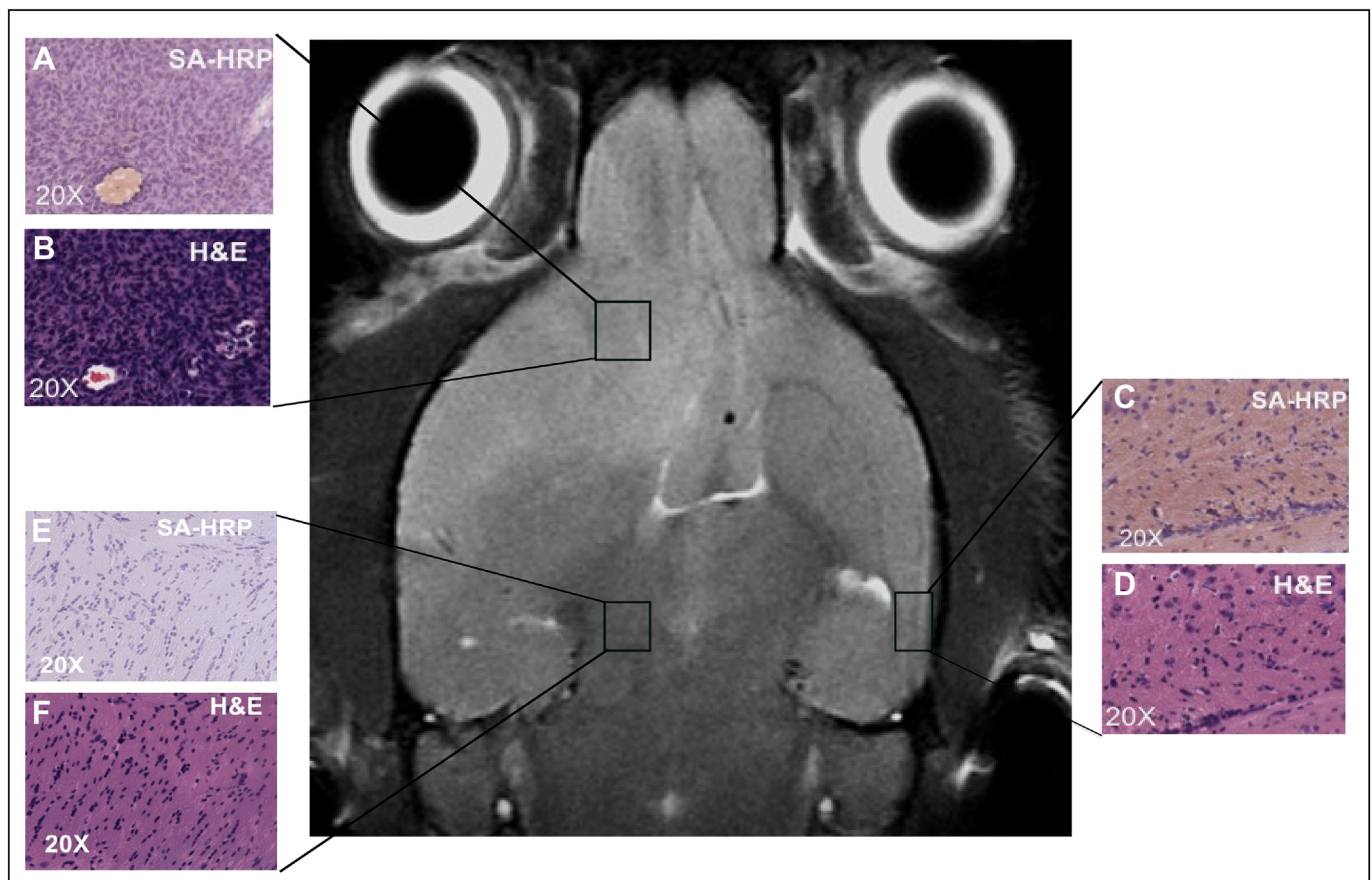


**Figure 6.** scFv fragment attached molecular probe was successful in reaching and targeting diffuse tumor regions not seen through MRI. (A, B) Top left region: Bulk tumor had traces of the scFv antibody attached-molecular probe as shown through SA-HRP (A), which were validated by H&E (B). (C, D) Bottom right region: The antibody attached-molecular probe was successful in reaching diffuse tumor regions, as shown through SA-HRP (C) and H&E (D) images. (E, F) Bottom left region: Comparative 'normal' brain regions [SA-HRP (E); H&E (F)].

## Discussion

Antibodies have become an important and a well-established class of drugs. Most recently, research has focused on scFvs as an alternative for larger whole antibody molecules. Therefore, scFvs have been developed against various targets for different cancers [34–37]. Furthermore, scFvs have been attached onto molecular targeting moieties for development of potential therapeutic and diagnostic applications using MRI and bioluminescence imaging [37–40].

Previous studies in our group have demonstrated that anti-ELTD1 treatments with commercial pAb have decreased tumor volumes and increased animal survival in both mouse GL261 and human G55 xenograft glioma models [26]. The aim of this study was to create and optimize an antibody therapy against ELTD1. We created a monoclonal and an scFv fragment of the mAb against the external region of ETLTD1. Regarding treatment response, both monoclonal and fragment antibody treatments were successful in increasing survival and decreasing tumor volumes. Although the fragment treatment against ELTD1 appeared to be successful, there was a high amount of variance seen within the tumor volumes and survival post tumor detection within the group, suggesting that, in future studies, we may need to optimize the fragment treatment plan because the scFv antibodies have a shorter life span compared to mAb and may need to be administered more frequently. Anti-ELTD1 therapy, both mAb and fragment anti-ELTD1, was successful in normalizing the perfusion levels within the tumor region. Both of the anti-ELTD1 treatments were successful in not only decreasing but also normalizing the MVD levels within the tumor region. This suggests that, by targeting ELTD1, we can normalize the tumor-related vasculature within the tumor region. While in previous reports we have shown a relationship between ELTD1 and VEGFR2 in GBM, this study works to shed some light on the relationship between ELTD1 and Notch, angiogenic marker, in GBM which was previously unknown [31]. Untreated G55 tumors were found to have increased Notch1 expression compared to contralateral healthy tissue. However, through repetitive treatments with both mAb and fragment against ELTD1, Notch1 expression levels decreased within the tumor. The decrease in Notch1 within the tumor may further explain and support the normalization of vasculature in the tumor.

By constructing biotin-albumin-Gd-DTPA molecular probes bound to either nonspecific IgG, monoclonal or fragment antibodies against ELTD1, we were not only able to localize our antibodies *in vivo* but were also able to quantify the signal intensity produced by the probes within the tumor region. Through this, we were able to determine that both the monoclonal and fragment anti-ELTD1 attached probes were successful in localizing within the tumor region. Furthermore, our molecular targeting data demonstrated that our anti-ELTD1 fragment attached probe was able to bind onto diffuse tumor regions that were once undetectable via MRI. This finding therefore suggests that our anti-ELTD1 fragment may be potentially used as a diagnostic method to localize diffuse tumors.

In conclusion, our molecular targeting data demonstrate the future diagnostic potential of our scFv antibody fragment against ELTD1 for distinguishing diffuse tumors that are undetectable through MRI. Both of our anti-ELTD1 treatments were successful in increasing survival, decreasing tumor volumes, and normalizing tumor associated vasculature. Although ELTD1 was shown to be downregulated through the Notch/Dll4 pathways in normal vasculature, this study sheds some light on the relationship between ELTD1 and Notch1 in GBMs. This study demonstrated that both our monoclonal and scFv antibody therapies against ELTD1 were effective and may be potential antiangiogenic therapies against GBMs.

## References

- [1] P.Y. Wen, S. Kesari, Malignant gliomas in adults, *N. Engl. J. Med.* 359 (2008) 492–507.
- [2] G. Karpel-Massler, U. Schmidt, A. Unterberg, M.E. Halatsch, Therapeutic inhibition of the epidermal growth factor receptor in high-grade gliomas: where do we stand? *Mol. Cancer Res.* 7 (2009) 1000–1012.
- [3] H. Ohgaki, P. Dessen, B. Jourde, S. Horstmann, T. Nishikawa, P.L. Di Patre, C. Burkhard, D. Schuler, N.M. Probst-Hensch, P.C. Maiorka, N. Baeza, P. Pisani, Y. Yonekawa, M.G.

- Yasargil, U.M. Lutolf, P. Kleihues, Genetic pathways to glioblastoma: a population-based study, *Cancer Res.* 64 (2004) 6892–6899.
- [4] C.J. Farrell, S.R. Plotkin, Genetic causes of brain tumors: neurofibromatosis, tuberous sclerosis, von Hippel-Lindau, and other syndromes, *Neurol. Clin.* 25 (2007) 925–946viii.
- [5] R. Stupp, W.P. Mason, M.J. van den Bent, M. Weller, B. Fisher, M.J. Taphoorn, K. Belanger, A.A. Brandes, C. Marosi, U. Bogdahn, J. Curschmann, R.C. Janzer, S.K. Ludwin, T. Gorlia, A. Allgeier, D. Lacombe, J.G. Cairncross, E. Eisenhauer, R.O. Mirimanoff, European Organisation for Research and Treatment of Cancer Brain Tumor and Radiotherapy Groups, National Cancer Institute of Canada Clinical Trials Group, Radiotherapy plus concomitant and adjuvant temozolomide for glioblastoma, *N. Engl. J. Med.* 352 (2005) 987–996.
- [6] C.Y. Lee, Strategies of temozolomide in future glioblastoma treatment, *Onco. Targets Ther.* 10 (2017) 265–270.
- [7] G.J. Kitange, B.L. Carlson, M.A. Schroeder, P.T. Grogan, J.D. Lamont, P.A. Decker, W. Wu, C.D. James, J.N. Sarkaria, Induction of MGMT expression is associated with temozolomide resistance in glioblastoma xenografts, *Neuro Oncol.* 11 (2009) 281–291.
- [8] H.S. Friedman, M.D. Prados, P.Y. Wen, T. Mikkelsen, D. Schiff, L.E. Abrey, W.K. Yung, N. Paleologos, M.K. Nicholas, R. Jensen, J. Vredenburg, J. Huang, M. Zheng, T. Cloughesy, Bevacizumab alone and in combination with irinotecan in recurrent glioblastoma, *J. Clin. Oncol.* 27 (2009) 4733–4740.
- [9] T.N. Kreisl, L. Kim, K. Moore, P. Duic, C. Royce, I. Stroud, N. Garren, M. Mackey, J.A. Butman, K. Camphausen, J. Park, P.S. Albert, H.A. Fine, Phase II trial of single-agent bevacizumab followed by bevacizumab plus irinotecan at tumor progression in recurrent glioblastoma, *J. Clin. Oncol.* 27 (2009) 740–745.
- [10] O.L. Chinot, W. Wick, W. Mason, R. Henriksson, F. Saran, R. Nishikawa, A.F. Carpenter, K. Hoang-Xuan, P. Kavan, D. Cernea, A.A. Brandes, M. Hilton, L. Abrey, T. Cloughesy, Bevacizumab plus radiotherapy-temozolomide for newly diagnosed glioblastoma, *N. Engl. J. Med.* 370 (2014) 709–722.
- [11] R.L. Jensen, M.L. Mumert, D.L. Gillespie, A.Y. Kinney, M.C. Schabel, K.L. Salzman, Pre-operative dynamic contrast-enhanced MRI correlates with molecular markers of hypoxia and vascularity in specific areas of intratumoral microenvironment and is predictive of patient outcome, *Neuro Oncol.* 16 (2014) 280–291.
- [12] S. Das, P.A. Marsden, Angiogenesis in glioblastoma, *N. Engl. J. Med.* 369 (2013) 1561–1563.
- [13] L. Poellinger, U. Lendahl, Modulating Notch signaling by pathway-intrinsic and pathway-extrinsic mechanisms, *Curr. Opin. Genet. Dev.* 18 (2008) 449–454.
- [14] A.C. Miller, E.L. Lyons, Herman TG. cis-Inhibition of Notch by endogenous Delta biases the outcome of lateral inhibition, *Curr. Biol.* 19 (2009) 1378–1383.
- [15] M. Masiero, F.C. Simoes, H.D. Han, C. Snell, T. Peterkin, E. Bridges, L.S. Mangala, S.Y. Wu, S. Pradeep, D. Li, C. Han, H. Dalton, G. Lopez-Berestein, J.B. Tuyenman, N. Mortensen, J.L. Li, R. Patient, A.K. Sood, A.H. Banham, A.L. Harris, F.M. Buffa, A core human primary tumor angiogenesis signature identifies the endothelial orphan receptor ELTD1 as a key regulator of angiogenesis, *Cancer Cell* 24 (2013) 229–241.
- [16] T. Nechiporuk, L.D. Urness, M.T. Keating, ETL, a novel seven-transmembrane receptor that is developmentally regulated in the heart. ETL is a member of the secretin family and belongs to the epidermal growth factor-seven-transmembrane subfamily, *J. Biol. Chem.* 276 (2001) 4150–4157.
- [17] R.A. Towner, R.L. Jensen, H. Colman, B. Vaillant, N. Smith, R. Casteel, D. Saunders, D.L. Gillespie, R. Silasi-Mansat, F. Lupu, C.B. Giles, J.D. Wren, ELTD1, a potential new biomarker for gliomas, *Neurosurgery* 72 (2013) 77–90discussion 91.
- [18] O. van Tellingen, B. Yetkin-Arik, M.C. de Gooijer, P. Wesseling, T. Wurdinger, H.E. de Vries, Overcoming the blood-brain tumor barrier for effective glioblastoma treatment, *Drug Resist. Updat.* 19 (2015) 1–12.
- [19] N.A. Buss, S.J. Henderson, M. McFarlane, J.M. Shenton, L. de Haan, Monoclonal antibody therapeutics: history and future, *Curr. Opin. Pharmacol.* 12 (2012) 615–622.
- [20] R. Razonnik, N. Novak, V. Curin Serbec, U. Rajcevic, Targeting malignant brain tumors with antibodies, *Front. Immunol.* 8 (2017) 1181.
- [21] Y. Lee, H. Kim, J. Chung, An antibody reactive to the Gly63-Lys68 epitope of NT-proBNP exhibits O-glycosylation-independent binding, *Exp. Mol. Med.* 46 (2014) e114.
- [22] O. Boussif, F. Lezoualc'h, M.A. Zanta, M.D. Mergny, D. Scherman, B. Demeneix, J.P. Behr, A versatile vector for gene and oligonucleotide transfer into cells in culture and *in vivo*: polyethylenimine, *Proc. Natl. Acad. Sci. U.S.A.* 92 (1995) 7297–7301.
- [23] J. Andris-Widhopf, C. Rader, P. Steinberger, R. Fuller, C.F. Barbas 3rd, Methods for the generation of chicken monoclonal antibody fragments by phage display, *J. Immunol. Methods* 242 (2000) 159–181.
- [24] C.F. Barbas, Phage display: a laboratory manual, Cold Spring Harbor Laboratory Press, Cold Spring Harbor, NY, 2001.
- [25] J. Han, J.H. Lee, S. Park, S. Yoon, A. Yoon, D.B. Hwang, H.K. Lee, M.S. Kim, Y. Lee, W.J. Yang, H.D. Youn, H. Kim, J. Chung, A phosphorylation pattern-recognizing antibody specifically reacts to RNA polymerase II bound to exons, *Exp. Mol. Med.* 48 (2016) e271.
- [26] J. Ziegler, R. Pody, P. Coutinho de Souza, B. Evans, D. Saunders, N. Smith, S. Mallory, C. Njoku, Y. Dong, H. Chen, J. Dong, M. Lerner, O. Mian, S. Tummala, J. Battiste, K.M. Fung, J.D. Wren, R.A. Towner, ELTD1, an effective anti-angiogenic target for gliomas: preclinical assessment in mouse GL261 and human G55 xenograft glioma models, *Neuro Oncol.* 19 (2017) 175–185.
- [27] W. Zhu, Y. Kato, D. Artemov, Heterogeneity of tumor vasculature and antiangiogenic intervention: insights from MR angiography and DCE-MRI, *PLoS One* 9 (2014), e86583.
- [28] R.A. Towner, N. Smith, S. Doblaz, P. Garteiser, Y. Watanabe, T. He, D. Saunders, O. Herlea, R. Silasi-Mansat, F. Lupu, *In vivo* detection of inducible nitric oxide synthase in rodent gliomas, *Free Radic. Biol. Med.* 48 (2010) 691–703.
- [29] H. Dafni, L. Landsman, B. Schechter, F. Kohen, M. Neeman, MRI and fluorescence microscopy of the acute vascular response to VEGF165: vasodilation, hyper-permeability and lymphatic uptake, followed by rapid inactivation of the growth factor, *NMR Biomed.* 15 (2002) 120–131.

- [30] G. Hermanson, Bioconjugate techniques, Academic Press, New York, 1996.
- [31] J. Ziegler, M. Zalles, N. Smith, D. Saunders, M. Lerner, K.M. Fung, M. Patel, J.D. Wren, F. Lupu, J. Battiste, R.A. Towner, Targeting ELTD1, an angiogenesis marker for glioblastoma (GBM), also affects VEGFR2: molecular-targeted MRI assessment, *Am. J. Nucl. Med. Mol. Imaging* 9 (2019) 93–109.
- [32] E. Haacke, Magnetic resonance imaging: physical principles and sequence design, Wiley-Liss, New York, 1999.
- [33] F. Serban, O. Daianu, L.G. Tataranu, S.A. Artene, G. Emami, A.M. Georgescu, O. Alexandru, S.O. Purcaru, D.E. Tache, M.M. Danculescu, V. Sfredel, A. Dricu, Silencing of epidermal growth factor, latrophilin and seven transmembrane domain-containing protein 1 (ELTD1) via siRNA-induced cell death in glioblastoma, *J. Immunoassay Immunochem.* 38 (2017) 21–33.
- [34] C.T. Kuan, N. Srivastava, R.E. McLendon, W.A. Marasco, M.R. Zalutsky, D.D. Bigner, Recombinant single-chain variable fragment antibodies against extracellular epitopes of human multidrug resistance protein MRP3 for targeting malignant gliomas, *Int. J. Cancer* 127 (2010) 598–611.
- [35] X. Zhu, S. Bidlingmaier, R. Hashizume, C.D. James, M.S. Berger, B. Liu, Identification of internalizing human single-chain antibodies targeting brain tumor sphere cells, *Mol. Cancer Ther.* 9 (2010) 2131–2141.
- [36] S.S. Patil, R. Railkar, M. Swain, H.S. Atreya, R.R. Dighe, P. Kondaiah, Novel anti IGFBP2 single chain variable fragment inhibits glioma cell migration and invasion, *J. Neurooncol.* 123 (2015) 225–235.
- [37] Z. Lu, K. Kamat, B.P. Johnson, C.C. Yin, N. Scholler, K.L. Abbott, Generation of a fully human scFv that binds tumor-specific glycoforms, *Sci. Rep.* 9 (2019) 5101.
- [38] C. Mazzocco, G. Fracasso, C. Germain-Genevois, N. Dugot-Senant, M. Figini, M. Colombatti, N. Grenier, F. Couillaud, In vivo imaging of prostate cancer using an anti-PSMA scFv fragment as a probe, *Sci. Rep.* 6 (2016), 23314.
- [39] L. Yang, H. Mao, Y.A. Wang, Z. Cao, X. Peng, X. Wang, H. Duan, C. Ni, Q. Yuan, G. Adams, M.Q. Smith, W.C. Wood, X. Gao, S. Nie, Single chain epidermal growth factor receptor antibody conjugated nanoparticles for in vivo tumor targeting and imaging, *Small* 5 (2009) 235–243.
- [40] M. Lariviere, C.S. Lorenzato, L. Adumeau, S. Bonnet, A. Hemadou, M.J. Jacobin-Valat, A. Noubhani, X. Santarelli, L. Minder, C. Di Primo, S. Sanchez, S. Mornet, J. Laroche-Traineau, G. Clofent-Sanchez, Multimodal molecular imaging of atherosclerosis: nanoparticles functionalized with scFv fragments of an anti-alphaIIbeta3 antibody, *Nanomedicine* 22 (2019), 102082.